Noise-induced amplitude and chirp jitter in dispersion-managed soliton communications

J. Nathan Kutz

Fondazione Ugo Bordoni, Via B. Castiglione 59, 00142 Rome, Italy

P. K. A. Wai

Department of Electronic Engineering, Hong Kong Polytechnic University, Hung Hom, Kowloon, Hong Kong, China

Received April 15, 1998

An analytic theory is presented that demonstrates that noise-induced amplitude and quadratic chirp jitter in a dispersion-managed soliton system can impose a fundamental transmission limit. Using a variational method, we show that the nonlinear amplitude and chirp dynamics are well approximated by a two-dimensional random-walk process. © 1998 Optical Society of America

OCIS codes: 260.2030, 110.4280.

Dispersion management has become increasingly important because of its excellent performance characteristics. As a result, growing research efforts have focused on the nonlinear pulse propagation dynamics of so-called dispersion-managed solitons.[1–5] Of particular importance is the interaction of the propagating soliton with the noise field that arises from the amplified spontaneous emission of the erbium-doped fiber amplifiers. It has been shown[6–10] that dispersion management reduces the Gordon–Haus timing jitter[11] by the power enhancement factor required to support the periodic dispersion-managed solitons.[1–5] In addition to timing jitter, the noise field can also induce significant amplitude and quadratic chirp jitter, leading to bit errors and a fundamental transmission limit when the pulse amplitude falls below the detection threshold of a receiver or the chirp is large at a detector. We present a variational description of the nonlinear amplitude and chirp dynamics when driven by a noise field and show that the resulting nonlinear dynamics can be well approximated by a simple two-dimensional (2-D) random-walk process for which its mean-square statistics can be evaluated. This description allows for an analytic calculation of the bit error rate associated with amplitude and chirp jitter and a comparison with the Gordon–Haus jitter penalty.

The evolution of the (slowly varying) electric-field envelope propagating in an optical fiber that includes noise, loss and gain fluctuations, a periodically varying dispersion, and the Kerr nonlinearity is governed by the dispersion-managed nonlinear Schrödinger equation

$$i\,\frac{\partial Q}{\partial Z} + \frac{\sigma(Z)}{2}\,\frac{\partial^2 Q}{\partial T^2} + a^2(Z)\,|Q|^2 Q = S(Z,T)\,, \qquad (1)$$

where Q is the envelope normalized by the initial peak field intensity $|E_0|^2$, T is the physical time normalized by $T_0/1.76$, T_0 is the FWHM intensity of the pulse, Z is the physical distance divided by the nonlinear length $Z_{\mathrm{NL}} = (\lambda_0 A_{\mathrm{eff}})/(2\pi n_2 |E_0|^2)$, $n_2 = 2.6 \times 10^{-16}$ cm^2/W is the nonlinear coefficient of the fiber, $A_{\mathrm{eff}} = 60\ \mu$m^2 is the effective cross-sectional area of the fiber, $\lambda_0 = 1.55\ \mu$m is the carrier's free-space wavelength, and c is the speed of light. Here $|S(Z,T)| \ll 1$ is a white-noise process and $a(Z)$ gives the loss–gain fluctuations, so $\mathrm{d}a/\mathrm{d}Z + \Gamma a = G\sum_{n=1}^{N}\delta(Z - nZ_a)a$, where Z_a is the normalized amplifier spacing, $\Gamma = 0.023$ km^{-1} is the loss rate (0.2 dB/km), $G = \exp(\Gamma Z_a)$ is the gain, N is the total number of amplifiers, and δ is the Dirac delta function (see Fig. 1). We take $\sigma(Z)$ to be the minimally deforming, symmetrized dispersion map[2] given by $\sigma(Z) = (\lambda_0{}^2 Z_{\mathrm{NL}})/[2\pi c(T_0/1.76)^2]D(Z)$, where

$$D(Z) = \begin{cases} D_- & 0 < Z < Z_-/2Z_{\mathrm{NL}} \\ D_+ & Z_-/2Z_{\mathrm{NL}} < Z < (Z_-/2 + Z_+)/Z_{\mathrm{NL}} \\ D_- & (Z_-/2 + Z_+)/Z_{\mathrm{NL}} < Z < P \end{cases}, \qquad (2)$$

$P = (Z_- + Z_+)/Z_{\mathrm{NL}}$, $D(Z) = D(Z + P)$ and $D_+ > 0 > D_-$ are the dispersion values in each segment of fiber, and $Z_\pm$ is the length of each fiber segment (see Fig. 1).

Because the pulses under consideration are far from idealized solitons, standard perturbation theories are inadequate to capture the dynamics inasmuch as the chirp is not described by the soliton perturbation equations. In contrast, the variational approach is

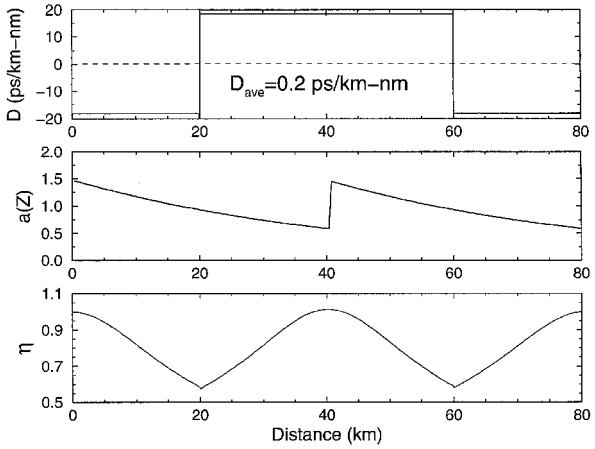

Fig. 1. Typical dispersion map (top) with loss-gain intensity fluctuations (middle) and average intensity fluctuations η (bottom).

0146-9592/98/131022-03$15.00/0

successful and accurate in capturing the essential features of the nonlinear dynamics.[2–4] The Lagrangian associated with Eq. (1) is

$$L = \int_{-\infty}^{\infty} \left[i\left(Q\,\frac{\partial Q^*}{\partial Z} - Q^*\,\frac{\partial Q}{\partial Z}\right) + \sigma(Z)\left|\frac{\partial Q}{\partial T}\right|^2 - a^2(Z)\,|Q|^4 + 2(SQ^* + S^*Q)\right] \mathrm{d}T\,. \tag{3}$$

For the pulse ansatz[2–4] we assume that

$$Q(Z,T) = \sqrt{\eta}\,\mathrm{sech}[\eta(T-C)]\exp\{i[\Omega(T-C) + \beta(T-C)^2 + (\phi/2)]\}, \tag{4}$$

where η, β, C, Ω, and ϕ are free parameters that depend on Z and correspond to amplitude, chirp, center position, frequency, and phase, respectively.

Variations of Eq. (3) with respect to the free parameters[2–4] give the coupled amplitude-chirp system:

$$\frac{\mathrm{d}\eta}{\mathrm{d}Z} = -2\sigma(Z)\beta\eta - (S_\beta/\pi^2)\,, \tag{5a}$$

$$\frac{\pi^2}{2}\,\frac{\mathrm{d}\beta}{\mathrm{d}Z} = \sigma(Z)\,(\eta^4 - \pi^2\beta^2) - a(Z)^2\eta^3 + (S_\eta/2)\,, \tag{5b}$$

which is decoupled from C and Ω (Refs. 6 and 8) and where

$$S_x = \frac{3\eta^3}{a(Z)}\int_{-\infty}^{\infty}\left[S(Z,T)\,\frac{\partial Q^*}{\partial x} + S(Z,T)^*\,\frac{\partial Q}{\partial x}\right]\mathrm{d}T \tag{6}$$

is the projection of the noise field on each of the evolution parameters. Note that for $S(Z,T) = 0$ the equations for the amplitude and the chirp reduce to those reported previously.[2,3]

As noted by Gordon and Haus,[11] a broadband (white) noise source excites all orthogonal modes with equal mean energies and with random uncorrelated phases. Here we assume that the ansatz in Eq. (4) is the ground state of the soliton modes. In this approximation the resulting orthogonal modes can be constructed from the adjoint operator of the linearized nonlinear Schrödinger equation.[12] Thus the noise-field phasor components that contribute to the amplitude and chirp dynamics are

$$S(Z,T) = \zeta\sum_{n=0}^{N}\delta(Z+nP)Q(Z,T)(is_1 + s_2 \times\{1 - \eta(T-C)\tanh[\eta(T-C)]\})\,, \tag{7}$$

where ζ represents the (real) strength of the noise term at each of the (identical) amplifiers and s_i are random variables assumed to be Gaussian distributed with mean zero and unit variance. We note that, for a typical experiment, $T_0 = 25$ ps, which gives $Z_{\mathrm{NL}} = 516$ km for the ideal, periodic solution.[2] Further, $D_+ = 17.4$ ps/(km nm) and $D_- = 17.0$ ps/(km nm), with $Z_+ = Z_- = Z_a = 40$ km, so the corresponding noise strength is $\zeta^2 \approx 0.0002$ (see, for example, Ref. 13).

In the absence of noise and at the critical value of the initial power enhancement,[1,2] the pulse undergoes a periodic evolution,[1–3] so at the end of a dispersion map period the pulse returns to the initial, chirp-free state $(\eta, \beta) = (1, 0)$. With noise, however, the dynamics in the η–β phase plane experiences a random, discrete jump at each amplifier location given by [substitute Eq. (7) into Eqs. (5) and (6)]

$$\eta_+ = \eta_- - \eta_- A_1\,, \qquad \beta_+ = \beta_- + \frac{3+\pi^2}{6}\,\eta_-{}^2 A_2\,, \tag{8}$$

where $\eta_\pm$ and $\beta_\pm$ are the amplitude and the chirp before and after an amplifier and $A_i = s_i\zeta/a_*$ is the noise strength determined by the amplified stimulated emission divided by a_* ($\approx$1), the value of $a(Z)$ at the amplifier. Between amplifiers, the amplitude and the chirp are completely described by Eqs. (5) with $S_x = 0$.

For illustrative purposes only, we take $\zeta^2 = 0.005$ and demonstrate in Fig. 2 the periodic pulse dynamics in the absence of noise (left) and a typical realization of the dynamics in the presence of noise (right). The light-gray curves are the amplitude-chirp fluctuations during a dispersion map period, whereas the dots (connected by solid curves) depict the location in the phase plane after every dispersion map period, i.e., the Poincaré section.[2] Thus the noise field causes the pulse to evolve (randomly) away from the ideal, periodic solution that corresponds to chirp-free, error-free transmission.

To quantify the effects of the noise-induced amplitude and chirp jitter, we measure the mean-square radial growth away from the $(\eta, \beta) = (1, 0)$ initial condition at the end of each dispersion map period by calculating $\langle R^2\rangle = \langle(\eta - 1)^2\rangle + \langle\beta^2\rangle$. We simplify the analysis by observing that Fig. 2 (right) resembles a 2-D random walk; i.e., the discrete jumps in η and β cause a random motion in the phase plane. We can then approximate the dynamics of Eqs. (5) and (8) by defining a 2-D random-walk process:

$$X_+ = X_- - A_1\,, \qquad Y_+ = Y_- + \frac{3+\pi^2}{6}\,A_2\,, \tag{9}$$

where $X_\pm$ and $Y_\pm$ are random-walk variables that correspond to η and β, respectively, and the jumps

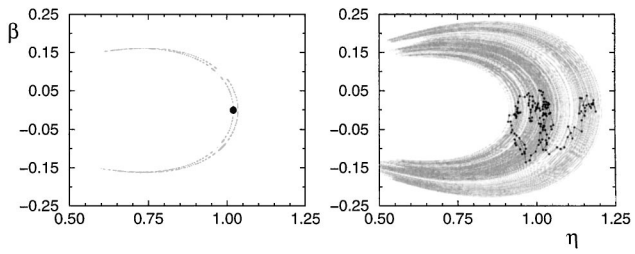

Fig. 2. Periodic phase-plane dynamics in the absence of the noise field (left) and a typical realization of amplitude-chirp dynamics and Poincaré section (dots) when driven by noise (right) for $\zeta^2 = 0.005$.

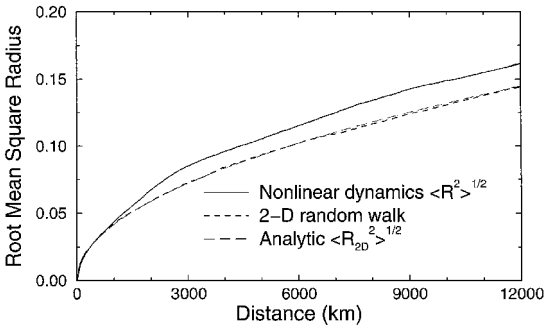

Fig. 3. Root-mean-square radial distance from starting values $(\eta, \beta) = (1, 0)$ for 8000 realizations and $\zeta^2 = 0.005$ for the nonlinear dynamics, the approximate 2-D random walk, and the analytic formula for the 2-D random walk.

occur at each amplifier in analogy to Eqs. (8). For such a random walk the mean-square radial growth of the pulse from the initial point $(X, Y) = (1, 0)$ is simply

$$\langle R_{2D}{}^2 \rangle = \left[\langle A_1{}^2 \rangle + \left(\frac{3 + \pi^2}{6} \right)^2 \langle A_2{}^2 \rangle \right] M , \qquad (10)$$

where M is the dispersion map periods traversed. We test the validity of the 2-D random-walk approximation by comparing in Fig. 3 the growth of the mean-square radius for the nonlinear evolution given by Eqs. (5) and (8), the approximation in Eqs. (9), and the analytic prediction given by Eq. (10). We note that the mean-square radial growth from Eqs. (5) and (8) grows approximately as the square root of distance traveled, agreeing reasonably well with the 2-D random-walk process of Eqs. (9). Even at 12,000 km the disagreement is only ≈15%.

From a system performance perspective, the random motion of the pulse in the η–β phase plane can impose transmission penalties in the following way: Either the amplitude η can drop below the detection threshold of the receiver or, alternatively, the chirp β can be large enough to degrade the performance of the detectors because of its spreading of the pulse spectrum, which is important because of filtering before detection in dense wavelength-division-multiplexed systems. As it is difficult to evaluate bit errors that are due to the chirp, we simply compare the amplitude jitter with the Gordon–Haus jitter[6–9] and evaluate the critical distance of propagation at which a bit error rate of 10^{-9} occurs for the realistic case of $\zeta^2 = 0.0002$. The Gordon–Haus penalty,[11] assuming that the detection window is four times the pulse width, can be evaluated when we note that[6] $\langle \delta T^2 \rangle = 4\zeta^2 L^3/27P$, so the critical distance is achieved at $L \approx 5.3$ (≈2700 km). Alternatively, a 10^{-9} bit error rate in a 1 that is due to amplitude jitter occurs when[14] $\langle \delta \eta^2 \rangle \approx [(I_1 - I_D)/5.9]^2$, where $I_1 - I_D$ measures the difference between the peak of a 1 and its detection threshold.[14] Approximating the amplitude jitter by the random walk in Eqs. (9) gives $\langle \delta \eta^2 \rangle \approx \langle X^2 \rangle = \zeta^2 L/P$. For an amplitude-detection window of $I_1 - I_D \approx 0.67$ (which is larger than the normal 0.5), the amplitude jitter contributes also at a critical distance of $L = 5.3$. Thus the amplitude jitter in this strongly dispersion-managed, physically realizable system is as important as the Gordon–Haus jitter. We note, however, that in practice it is difficult to distinguish between an error that is due to Gordon–Haus timing jitter and one that is due to amplitude jitter from an eye diagram or detector, thus making it difficult to separate the two effects. Further, for longer distances, the Gordon–Haus jitter grows much faster because of its L^3 dependence. Finally, we should point out that careful comparisons between the variational formalism and governing equation (1) have been shown to be highly accurate in predicting the pulse dynamics,[2–5] even in the presence of noise.[6–9] Thus the results here, although they are approximate, are quantitatively and qualitatively accurate representations of the resulting dispersion-managed dynamics.

In conclusion, we have shown that amplified stimulated emission noise induces amplitude and quadratic chirp jitter that can result in a fundamental transmission penalty of the same order as the Gordon–Haus timing jitter. By the variational method, a reduced, coupled nonlinear system of equations is found that can be well approximated by a simple 2-D random-walk process for which the growth of the mean-square radius from the ideal periodic, chirp-free solution can be easily calculated. This then provides a valuable method for understanding the noise-induced amplitude and chirp jitter and determining roughly the transmission penalties other than Gordon–Haus timing jitter that arise.

J. N. Kutz acknowledges several helpful discussions with S. G. Evangelides, Jr., M. Midrio, D. Muraki, J. Bronski, and J. P. Gordon and support from a National Science Foundation–NATO Fellowship (DGE-9710834). His present address is Department of Applied Mathematics, University of Washington, Seattle, Washington 98195-2420.

References

1. N. J. Smith, N. J. Doran, F. M. Knox, and W. Forysiak, Opt. Lett. **21,** 1981 (1996).
2. J. N. Kutz, P. Holmes, S. G. Evangelides, and J. P. Gordon, J. Opt. Soc. Am. B **15,** 87 (1998).
3. I. Gabitov, E. G. Shapiro, and S. K. Turitsyn, Opt. Commun. **134,** 317 (1997).
4. V. Grigoryan, T. Yu, E. Golovchenko, C. Menyuk, and A. Pilipetskii, Opt. Lett. **22,** 1609 (1997).
5. T. Georges, Opt. Lett. **22,** 679 (1997).
6. J. N. Kutz and P. K. A. Wai, IEEE Photon. Technol. Lett. **10,** 702 (1998).
7. S. Kumar and F. Lederer, Opt. Lett. **22,** 1870 (1997).
8. T. Okamawari, A. Maruta, and Y. Kodama, in *New Trends in Optical Soliton Transmission Systems,* A. Hasegawa and M. Shinomiya, eds. (Kluwer, Dordrecht, The Netherlands, to be published).
9. G. M. Carter, J. M. Jacob, C. R. Menyuk, E. A. Golovchenko, and A. N. Pilipetskii, Opt. Lett. **22,** 513 (1997).
10. N. J. Smith, W. Forysiak, and N. J. Doran, Electron. Lett. **32,** 2085 (1996).
11. J. P. Gordon and H. A. Haus, Opt. Lett. **11,** 665 (1986).
12. M. I. Weinstein, SIAM J. Math. Anal. **16,** 472 (1985).
13. A. Mecozzi, J. Lightwave Technol. **16,** 37 (1998).
14. G. Agrawal, *Optical Fiber Communications* (Wiley, New York, 1992), Chap. 4.